Carbohydrate Polymers 86 (2011) 753–759

Contents lists available at ScienceDirect

Carbohydrate Polymers

journal homepage: www.elsevier.com/locate/carbpol

Removal of copper(II) from aqueous solution in fixed-bed column by carboxylic acid functionalized deacetylated konjac glucomannan

Xuegang Luo*, Feng Liu, Zaifang Deng, Xiaoyan Lin

Engineering Research Center of Biomass Materials of Education Ministry, Southwest University of Science and Technology, Mianyang, Sichuan 621010, China

ARTICLE INFO

Article history:
Received 16 March 2011
Received in revised form 22 April 2011
Accepted 16 May 2011
Available online 23 May 2011

Keywords:
Carboxylic acid functionalized deacetylated konjac glucomannan
Thermoforming
Copper
Column study

ABSTRACT

Carboxylic acid functionalized deacetylated konjac glucomannan (CADKGM) with regular cylinder shape was thermoplastically prepared by a single screw extruder. Thermoplastic deacetylated konjac glucomannan (TDKGM) using for preparation of CADKGM adsorbent showed good rheological processing properties with equilibrium torque of 13.1 N m and plasticizing time of 26 s at 160 °C, which was close to high density polyethylene (HDPE). The scanning electron micrograph results showed that CADKGM was porous inside the structure of the adsorbent. The removal of copper by CADKGM was studied in fixed-bed column. A comprehensive study was conducted to determine the breakthrough curves with varying bed heights, flow rates and initial concentrations. The breakthrough data gave a good fit to Thomas model. The consecutive adsorption–desorption cycles were applied to investigate the reusability of CADKGM. The adsorbed copper ions on CADKGM were easily desorbed by 0.01 mol L^{-1} HCl solution with desorption efficiency of 98%. The column capacity of CADKGM was not affected by an increase of reusable time.

1. Introduction

Agricultural field irrigated with heavy metal contaminated water causes a serious public health problem since many heavy metals can concentrate and accumulate in human body through food chain (Nayek, Gupta, & Saha, 2010; Wei & Yang, 2010; Wu, Tseng, & Juang, 2010). It is well acknowledged that toxic heavy metal ions are among the most poisonous pollutants in wastewater, which cannot be biodegraded or destroyed by any treatment process (Li, Wang, Allinson, Li, & Xiong, 2009; Liu, Yang, et al., 2009; Lu, Wang, Lei, Huang, & Zhai, 2009; Peng, Song, Yuan, Cui, & Qiu, 2009; Shi, Shao, Li, Shao, & Du, 2009; Sunarso & Ismadji, 2009). Copper ions are commonly found in industrial effluents such as mining, electroplating and battery manufacturing drainage. Copper is an essential element and plays an essential role in the human diet. However, acute doses can cause health problem such as nausea, vomiting and abdominal pain. Long-term exposure to higher than 0.5 mg L^{-1} of copper in natural water may cause liver damage. Moreover, copper in the dissolved form is potentially very toxic to aquatic plants and animals. From the environmental and public health point of view, it is important to effectively remove copper ions from the industry wastewaters before discharging. Many treatment processes, including chemical precipitation, ion-exchange, coagulation-flocculation, membrane filtration and adsorption, are used to remove heavy metal ions of polluted water (Babel & Kurniawan, 2003; El Samrani, Lartiges, & Villieras, 2008; Matlock, Howerton, & Atwood, 2002; Pehlivan & Altun, 2007; Sang, Gu, Sun, Li, & Liang, 2008). Among the treatment processes, the biosorption process using natural materials or waste products as adsorbents to remove heavy metal ions from wastewater is one of the most popular and effective processes (Bailey, Olin, Bricka, & Adrian, 1999; Demirbas, 2008; Farooq, Kozinski, Khan, & Athar, 2010; Sud, Mahajan, & Kaur, 2008; Vijayaraghavan & Yun, 2008; Wan Ngah, Teong, & Hanafiah, 2011; Wang & Chen, 2009). Compared with conventional treatment methods, the advantages of biosorption process lie in its low-cost and high removal efficiency. The concentration of heavy metal ions can be reduced to very low levels after the wastewater is treated by biosorption process.

In order to improve adsorption capacity of biosorbents, chemical modification is widely used (Wu, Kang, et al., 2010), including a direct chemical modified method and grafting of functional group chains on matrix biopolymer (O'Connell, Birkinshaw, & O'Dwyer, 2008). Modified biosorbents would be of great importance and be hoped for removal of heavy metal ions from wastewater in actual application. However, related literatures concerning concrete steps of applying modified biosorbents to practice are seldom found. The major reason is that many kinds of modified biosorbents are hard to be prepared or processed on a large scale. Moreover, many kinds of modified biosorbents have poor mechanical strength with high water absorbency, which cannot meet the industrial application requirements.

It was reported in our previous study that chemical modified konjac glucomannan by grafting hydrophobic monomers onto its backbone could be processed by thermoplastic extrusion (Xu, Luo,

* Corresponding author. Tel.: +86 08166089009; fax: +86 08166089009.
E-mail addresses: lxg-2007@163.com, lxg@swust.edu.cn (X. Luo).

0144-8617/$ – see front matter.
doi:10.1016/j.carbpol.2011.05.020

Lin, Zhuo, & Liang, 2009). It was further reported in a batch adsorption study that carboxylic acid functionalized deacetylated konjac glucomannan as a weak acid cation adsorbent showed relatively high adsorption capacity for removal of copper ion and lead ion from aqueous solution (Liu, Luo, Lin, Liang, & Chen, 2009). In order to prepare and process konjac glucomannan based adsorbent with relatively high mechanical strength on a large scale, carboxylic acid functionalized deacetylated konjac glucomannan (CADKGM) with regular cylinder shape was thermoplastically extruded and prepared by single screw extruder with subsequent chemical activation by sodium hydroxide. The main objective of this study was to investigate the copper ions removal efficiency and adsorption capacity of CADKGM adsorbent in fixed-bed column. Effects of various parameters on breakthrough curves were conducted. Thomas model was applied to fit the results obtained from the column study.

2. Experimental

2.1. Materials and instruments

The following chemicals including methyl acrylate (MA), methyl methacrylate (MMA), ammonium persulfate, alcohol, sodium hydroxide, hydrochloric acid, copper sulfate used in this work were all of analytical grade and obtained from Chengdu Kelong Chemicals Company. Refined KGM flour (50–150 μm) was purchased from Mianyang Anxian Dule Company and was used without further purification. High density polyethylene (HDPE) was purchased from Shanghai Secco Petrochemical Company.

The following instruments were used in this study: torque rheometer and single screw extruder (XSS-300, Shanghai Kechuang Rubber Machinery Co., Ltd.), atomic adsorption spectrometer (AA700, PE), scanning electron micrograph (S440, Leica Cambridge Ltd.), and peristaltic pump (BT-100, Shanghai Qingpu Huxi Instrument Factory).

2.2. Preparation of DKGM

KGM flour (200.0 g) and sodium hydroxide (15.0 g) were dispersed in 960 mL alcohol/water mixture solution (400:560 v/v) in a three-necked round-bottomed flask (2000 mL) equipped with a mechanical stirrer. The reaction mixture was stirred at a temperature of 50 °C for 2 h. As a result, deacetylated konjac glucomannan (DKGM) was obtained. DKGM powder was filtered out and washed with distilled water, and then was dried at 60 °C for further graft copolymerization experiment.

2.3. Synthesis of TDKGM

A mixture of 45.0 g of dried DKGM and 1200 mL of distilled water was stirred mechanically at 25 °C for 30 min in a three-necked round-bottomed flask (2000 mL) under nitrogen atmosphere. This treatment was followed by the addition of 120 mL of MA and 80 mL of MMA. Copolymerization was carried out at 75 °C for 3 h by adding ammonium persulfate (6.85 g) into the mixed solution. After 3 h, thermoplastic deacetylated konjac glucomannan (TDKGM) was filtered out of reacted system and washed thoroughly with distilled water and then refluxed with hot water for 12 h in order to remove any homopolymers that may be attached to the surface of TDKGM powder. The copolymer sample (TDKGM) was dried to a constant weight (175.0 g) at 50 °C. The graft percentage was determined by the following equation:

$$\text{Graft}\ \ (\%) = \frac{W_g - W_o}{W_o} \times 100 \qquad (1)$$

where W_o and W_g represent the initial weight and the graft weight of DKGM, respectively. The graft percentage of TDKGM was calculated as 289%.

2.4. Thermoplastic extrusion of TDKGM

Processing of the TDKGM was performed using a single screw extruder. The applied temperature during extrusion was kept at 160 °C. The extruder speed was kept at 40 rpm in all cases. Unifilar TDKGM was extruded through nozzles with a diameter of 1.25 mm. Unifilar TDKGM was cut into short cylinder pieces with length of 5 mm by granulator.

2.5. Chemical activation of TDKGM for CADKGM adsorbent

Short cylinder pieces of TDKGM were chemically activated under alkali condition using sodium hydroxide as follows: short cylinder pieces of TDKGM (200.0 g) were immersed in 500 mL of sodium hydroxide aqueous solution with the concentration of 10 wt%. The mixture was agitated at 50 °C for 12 h. The chemically activated TDKGM was neutralized by hydrochloric acid and collected by filtration and washed with distilled water. The product of CADKGM adsorbent was then dried at 60 °C.

2.6. Fixed-bed column experiments

Fixed-bed column experiments were conducted using a column with 3.0 cm internal diameter and 30 cm length. The column was packed with short cylinder pieces of CADKGM between two supporting layers of glass wool. The column was charged with Cu^{2+} aqueous solution in the up flow mode. Temperature was maintained at 15 °C. The column studies were performed at pH 5. A Perkin-Elmer-AA700 atomic absorption instrument was used in the determination of Cu^{2+} concentration of effluent by line's calibration curve.

The adsorption–desorption cycle experiments were carried out in a column with a bed height of 14 cm. The Cu^{2+} ion solution of 50 mg L^{-1} was fed through the bed in up-flow mode at 10 mL min^{-1} flow rate. Operation of the column was stopped when the effluent Cu^{2+} ion concentration reached a constant value. The Cu-loaded CADKGM was regenerated by using 0.01 mol L^{-1} hydrochloride. Hydrochloride was fed through the bed in up-flow mode at 8 mL min^{-1} flow rate until the effluent Cu^{2+} ion concentration reached a lowest value. The regenerated CADKGM was neutralized by 0.01 mol L^{-1} sodium hydroxide until the pH value in the effluent achieved a value of 6, and then deionised water was used to wash the bed for 5 h at a flow rate of 10 mL min^{-1}. The regenerated column was employed in the next adsorption cycle to investigate the reusability of CADKGM.

2.7. Characterization of TDKGM and CADKGM

A torque rheometer (XSS-300, Shanghai Kechuang Rubber Machinery Co., Ltd.) was used to study the effect of processing temperature on rheological processing properties of TDKGM. The processing temperature was set at 120 °C, 140 °C and 160 °C. The processing speed was kept at 40 rpm in all cases. The sample of TDKGM or HDPE with amount of 45.0 g was added into in an internal mixer at setting temperature. Various processing parameters could be obtained from the torque curves.

The morphologies of TDKGM and CADKGM were investigated by SEM (S440, Leica Cambridge Ltd.). All dried samples were sputter coated with gold prior to examination.

Water absorbency of the samples was determined as follows: 1.0 g of dry sample was added into a centrifuge tube (100 mL) containing 50 mL of distilled water. The sample was allowed to swell

thoroughly for 12 h. The sample was then centrifuged at 3000 rpm for 30 min. After removing the supernatant water, the sample was weighed. The weight difference was calculated as the amount of water absorbed in the sample. All experiments were conducted in triplicate. The average of the three water absorbency was used in the discussion.

2.8. Analysis of column data

In order to determine the operation and dynamic response of adsorption column, the bed breakthrough time (t_b, the time at which the ratio of C_t/C_o is 0.1) and bed exhaustion time (t_e, the time at which the ratio of C_t/C_o is 0.9) were used to evaluate the breakthrough curves. C_o is the inlet Cu^{2+} ion concentration and C_t is the outlet Cu^{2+} ion concentration. The equilibrium column capacity (q_e, mg g^{-1}) for a given feed concentration and flow rate is equal to the area under the plot of the adsorbed Cu^{2+} concentration ($C_{ad} = C_o - C_t$, mg L^{-1}) versus time (h) and is calculated as follow:

$$q_e = \frac{QA \times 60}{m_s \times 1000} = \frac{Q \times 60}{m_s \times 1000} \int_{t=0}^{t=t_{total}} C_{ad}\ dt \quad (2)$$

where t_{total}, Q, m_s and A are the total flow time (h), flow rate (mL min^{-1}), the total dry weight of CADKGM in column (g) and the area under the breakthrough curve, respectively.

3. Results and discussion

3.1. Effect of processing temperature

TDKGM with a glass transition temperature of 56.7 °C was synthesized by free radical graft copolymerization of methyl acrylate (MA) and methyl methacrylate (MMA) onto the backbone of deacetylated konjac glucomannan. DKGM is not able to soften and just decompose at much higher temperature. After grafting co-poly-MA-MMA onto the backbone of DKGM, TDKGM will soften when processing temperature is just higher than glass transition temperature of TDKGM. The molecular structure of TDKGM is the rigid-chain copolymer, which indicates that rheological behavior of TDKGM depends strongly on processing temperature. The torque curves of TDKGM thermoplastically processed at various temperatures were shown in Fig. 1. Torque rheological parameters of TDKGM including maximum torque, equilibrium torque and plas-

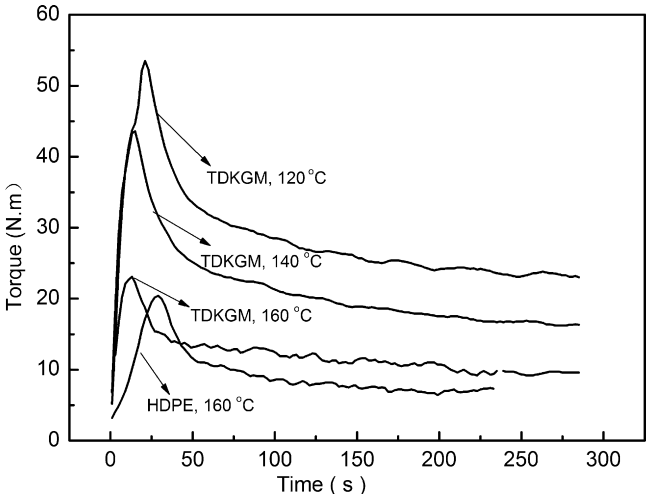

Fig. 1. Torque curves of TDKGM and HDPE.

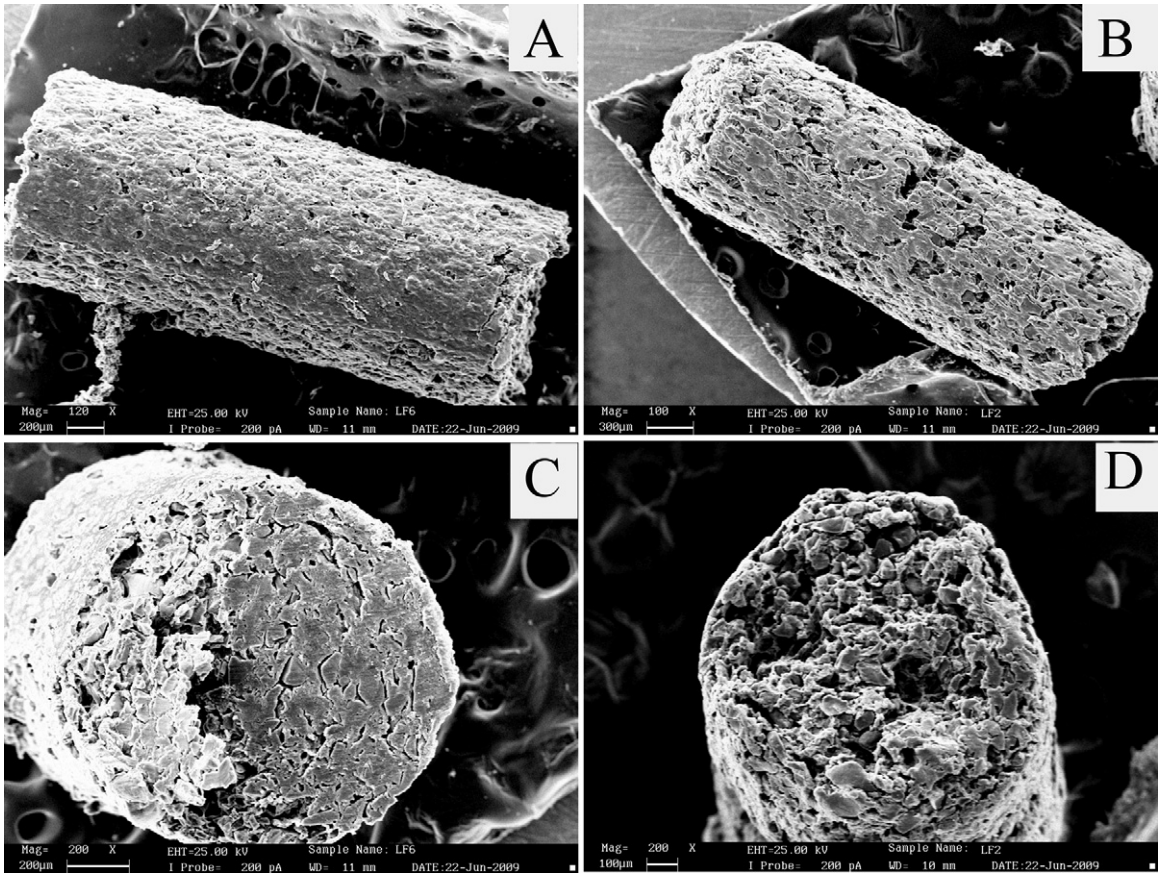

Fig. 2. SEM analysis of CADKGM adsorbent before and after alkali treatment.

Table 1
Torque rheological parameters at different temperatures.

Parameters	TDKGM (120 °C)	TDKGM (140 °C)	TDKGM (160 °C)	HDPE (160 °C)
Maximum torque (N m)	53.5	43.6	23.1	20.4
Equilibrium torque (N m)	30.6	23.5	13.1	11.1
Plasticizing time (s)	50	48	26	24

ticizing time were regularly reduced with increase of processing temperature as listed in Table 1. The torque curve of TDKGM at temperature of 160 °C was close to the torque curve of HDPE at the same temperature. It indicated that TDKGM showed good thermoplastic processing behavior and TDKGM can be easily extruded in a screw extruder.

3.2. SEM analysis

The SEM micrographs of TDKGM adsorbent before and after alkali treatment are shown in Fig. 2. The micrograph in Fig. 2(A) represents compact cylinder structure of TDKGM adsorbent with a diameter of 1.5 mm before alkali treatment. The section of TDKGM shown in Fig. 2(C) is in a few cases rough and scaly, which is helpful to chemical activation. When TDKGM adsorbent was suspended in alkali solution, the surface ester functionality of TDKGM can be easily hydrolyzed into CADKGM containing carboxyl groups. The SEM micrographs in Fig. 2(B) and (D) show the presence of pores inside the CADKGM adsorbent after alkali treatment. Porous structure of TDKGM can provide enough contacting sites that solutes in aqueous solution can easily exchange with functional groups. The water absorbency of TDKGM before alkali treatment was determined as 0.3 g H_2O/g TDKGM. After the sample was treated by alkali solution, the water absorbency of CADKGM adsorbent increased to 3.0 g H_2O/g CADKGM.

3.3. Effect of flow rate

The effect of flow rate on removal of Cu^{2+} ions from aqueous solution by CADKGM was investigated by varying the flow rate from 5 to 15 mL min^{-1} shown in Fig. 3. The amount of CADKGM packed in the column was 15.0 g. The bed height and initial Cu^{2+} concentration were kept at 21 cm and 50 mg L^{-1}, respectively. With the increase of flow rate from 5 mL min^{-1} into 15 mL min^{-1}, the column breakthrough time was reduced from 7.0 h to 1.0 h and the column capacity was decreased from 14.1 mg g^{-1} to 12.1 mg g^{-1}, respectively. The reduction of adsorption behavior with increasing

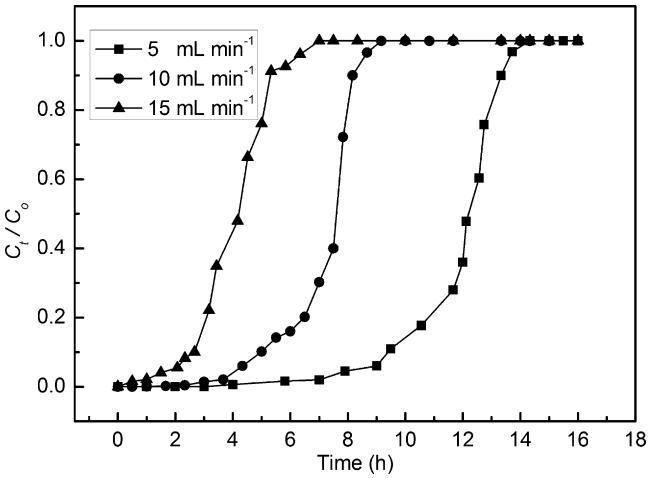

Fig. 3. Effect of flow rate on breakthrough curves.

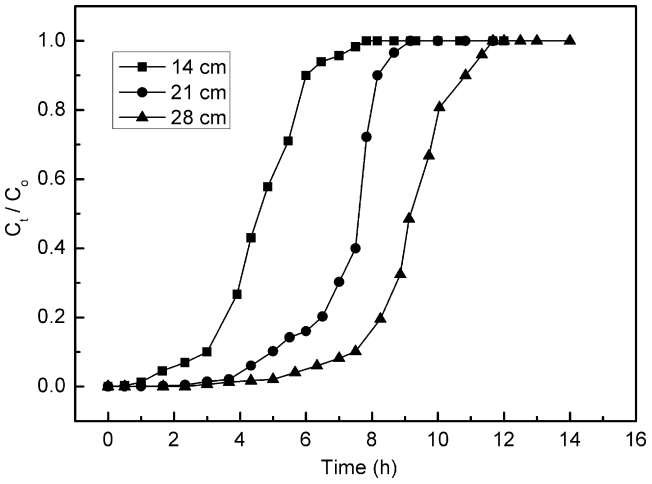

Fig. 4. Effect of bed height on breakthrough curves.

flow rate was due to the decrease of the contact time at higher flow rate (Ahmed, 2011). Cu^{2+} ions have enough time to diffuse into the pores of CADKGM through intra-particle diffusion at lower flow rate and more available functional group sites are able to capture Cu^{2+} ions around or inside the adsorbent. The breakthrough curve became steeper as the flow rate increased. It indicated that the equilibrium column capacity of CADKGM quickly reached its maximum value at higher flow rate because of more Cu^{2+} ions exchanging with functional group sites in shorter time.

3.4. Effect of bed height

Quantity of adsorbent inside the column is an important parameter in evaluating the performance of adsorption for continuous treatment. In order to yield different bed heights, 10 g, 15 g and 20 g of CADKGM were added to produce bed heights of 14 cm, 21 cm, and 28 cm, respectively. The breakthrough curves obtained by varying the bed heights from 14 cm to 28 cm at 10 mL min^{-1} flow rate and 50 mg L^{-1} initial Cu^{2+} concentration are presented in Fig. 4. It was observed that the breakthrough time and exhaustion time increased with increasing the bed height. The increase of breakthrough time and exhaustion time in adsorption with increasing bed depth was due to the increase in CADKGM doses, which provide greater functional sites for Cu^{2+} ions. Moreover, contact time is another important parameter affecting removal efficiency. When the column was packed at a lower bed height, Cu^{2+} ions had not enough contact time to diffuse inside the adsorbent, which led to reduction of breakthrough time and removal efficiency. The uptake became less effective. With increase of the bed height from 14 into 28 cm, the breakthrough time have evidently prolonged from 3.0 h to 7.2 h. The column showed good performance to remove Cu^{2+} ions from the fluid with high removal efficiency of 99.7%. The equilibrium column capacity improved from 12.6 mg g^{-1} to 13.5 mg g^{-1} when the bed height increased from 14 cm to 28 cm.

In order to predict the relationship between bed depth and service time at fixed adsorption conditions, the linear bed depth service time (BDST) model was used to analyze the data. The linear BDST equation can be expressed as follows (Bohart & Adams, 1920; Futalan, Kan, Dalida, Pascua, & Wan, 2011; Kumar & Bandyopadhyay, 2006):

$$t = \frac{N_o Z}{C_o v} - \frac{1}{K_a C_o} \ln\left(\frac{C_o}{C_b} - 1\right) \quad (3)$$

where C_o is the initial Cu^{2+} concentration, C_b is the breakthrough Cu^{2+} concentration (mg L^{-1}) when the effluent concentration reaches to 5 mg L^{-1}, N_o is the adsorption capacity (mg L^{-1}), v is the

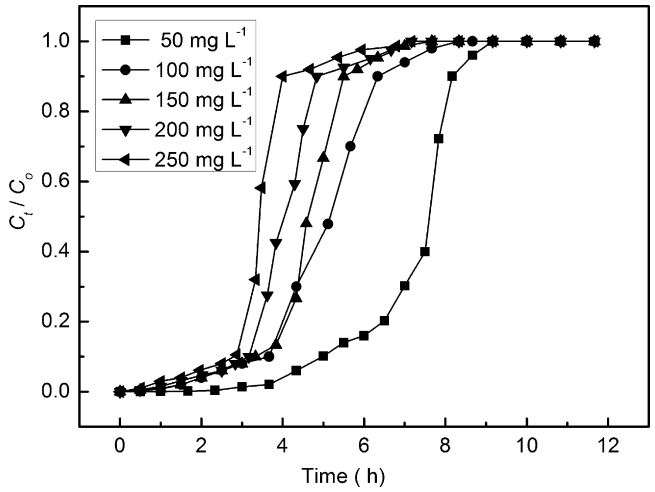

Fig. 5. Effect of initial concentration on breakthrough curves.

linear flow velocity of Cu^{2+} solution through the bed calculated by dividing the flow rate by the column section area (cm h^{-1}), Z is the bed depth of column (cm), t is the service time (h) when the normalized concentration (C_t/C_o) reaches to 0.1 and k_a is the rate constant (L mg^{-1} h^{-1}).

The plot of service time versus bed height was linear with high correlation coefficient of 0.999. It suggested that BDST model well fitted the data. The BDST model parameters are useful to scale up the column adsorption process for different bed heights without further experiment. The values of BDST model parameters were calculated from the slope and intercept of the plot. The values of N_o and K_a were 1273.89 mg L^{-1} and 0.036 L mg^{-1} h^{-1}, respectively. The values of N_o and K_a suggested that CADKGM has high efficiency for removal of Cu^{2+} from aqueous solution. By setting service time $t = 0$ and solving for Z in the above equation, the minimum bed height (Z_{min}) is obtained as 4.1 cm. The parameter of minimum bed height reflects the shortest bed height needed to reach the breakthrough concentration at service time $t = 0$.

3.5. Effect of initial concentration

The column performance of CADKGM was conducted at various inlet Cu^{2+} ion concentrations. The breakthrough curves obtained by changing inlet Cu^{2+} ion concentration from 50 mg L^{-1} to 250 mg L^{-1} at 10 mL min^{-1} and 21 cm bed height are presented in Fig. 5. It is clear that CADKGM can be quickly saturated at the higher initial concentration, which leads to reduction of the breakthrough time with increase of initial concentration. The equilibrium column capacity obtained by experiment increased from 14.1 mg g^{-1} to 35.0 mg g^{-1} when the initial concentration increased from 50 mg L^{-1} to 250 mg L^{-1}. The maximum equilibrium column capacity of 35.0 mg g^{-1} was similar to the equilibrium adsorption capacity of CADKGM determined from in our batch study at the initial concentration of 250 mg L^{-1}. A higher column capacity can be achieved at a higher Cu^{2+} ions concentration due to the higher driving force. The driving force for adsorption is the concentration difference between the solute on the adsorbent and the solute in the solution. The driving force between the Cu^{2+} ions on CADKGM and the Cu^{2+} ions in the solution could be improved with increasing Cu^{2+} ions concentration.

3.6. Application of Thomas model

The adsorption data from the column studies at various flow rates and initial concentrations were analyzed using the Thomas model. Thomas model was based on two assumptions. The first assumption is Langmuir kinetics of adsorption–desorption without axial dispersion. The second assumption is that the rate driving force in adsorption process conforms to second order reversible reaction kinetics. It is used to predict the maximum column capacity of CADKGM. The linear Thomas model has the following form (Kose & Ozturk, 2008; Qaiser, Saleemi, & Umar, 2009; Tabakci & Yilmaz, 2008):

$$\ln\left(\frac{C_o}{C_t} - 1\right) = \frac{K_{Th} q_e M_s}{Q} - K_{Th} C_o t \quad (4)$$

where K_{Th} is the Thomas rate constant (mL min^{-1} mg^{-1}), q_e is the maximum column capacity (mg g^{-1}), M_s is the mass of adsorbent (g), Q is the flow rate (mL min^{-1}), C_o is the inlet Cu^{2+} ion concentration and C_t is the outlet Cu^{2+} ion concentration any time (t, min). The Thomas model was fitted to the column data at C_t/C_o ratio higher than 0.05 and lower than 0.95 to investigate the breakthrough behavior of Cu^{2+} ion onto CADKGM. The values of K_{Th} and q_e can be calculated from a plot $\ln(C_o/C_t - 1)$ versus t at a given condition listed in Table 2. The Thomas model well fitted the experimental data at various flow rates and initial inlet concentrations with R^2 values higher than 0.95. Moreover, the maximum column capacity calculated from the Thomas model ($q_{e,cal}$, mg g^{-1}) is very close to the experimental column capacity ($q_{e,exp}$, mg g^{-1}).

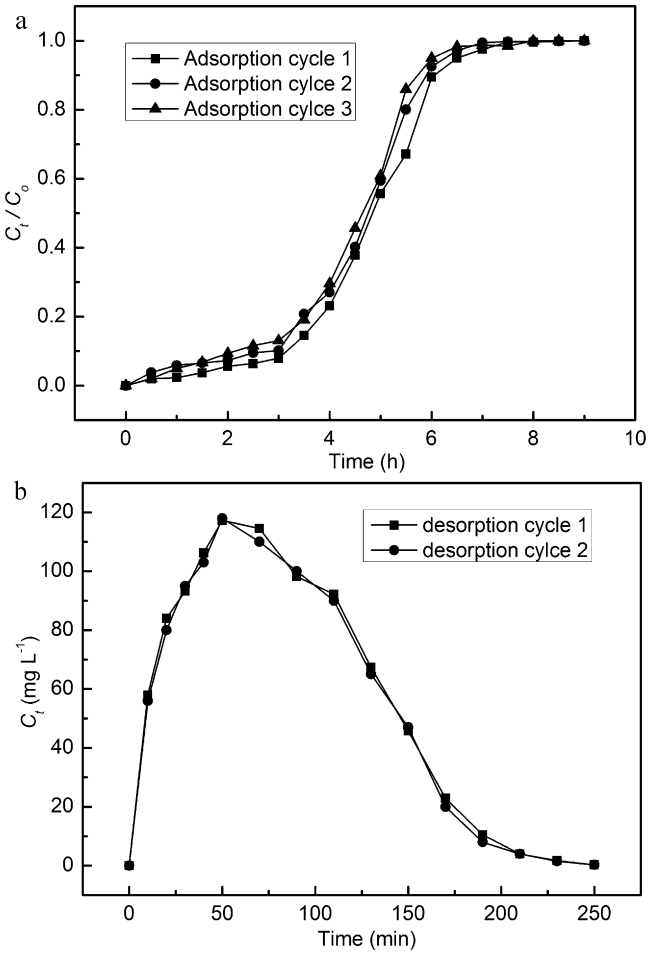

Fig. 6. Adsorption–desorption cycles of Cu^{2+} ions onto CADKGM.

3.7. Column regeneration and reuse studies

The adsorption–desorption cycle was repeated three times for the same column. The breakthrough curves for each adsorption

Table 2
Thomas model parameters.

C_o (mg L^{-1})	Q (mL min^{-1})	K_{Th} (mL mg^{-1} min^{-1})	$q_{e,exp}$ (mg g^{-1})	$q_{e,cal}$ (mg g^{-1})	R^2
50	5	0.188	14.1	13.96	0.98
50	10	0.324	13.5	13.67	0.98
50	15	0.386	12.1	12.86	0.97
100	10	0.218	19.8	19.7	0.98
150	10	0.187	27.7	27.3	0.96
200	10	0.149	31.7	32.6	0.96
250	10	0.103	35.0	35.5	0.95

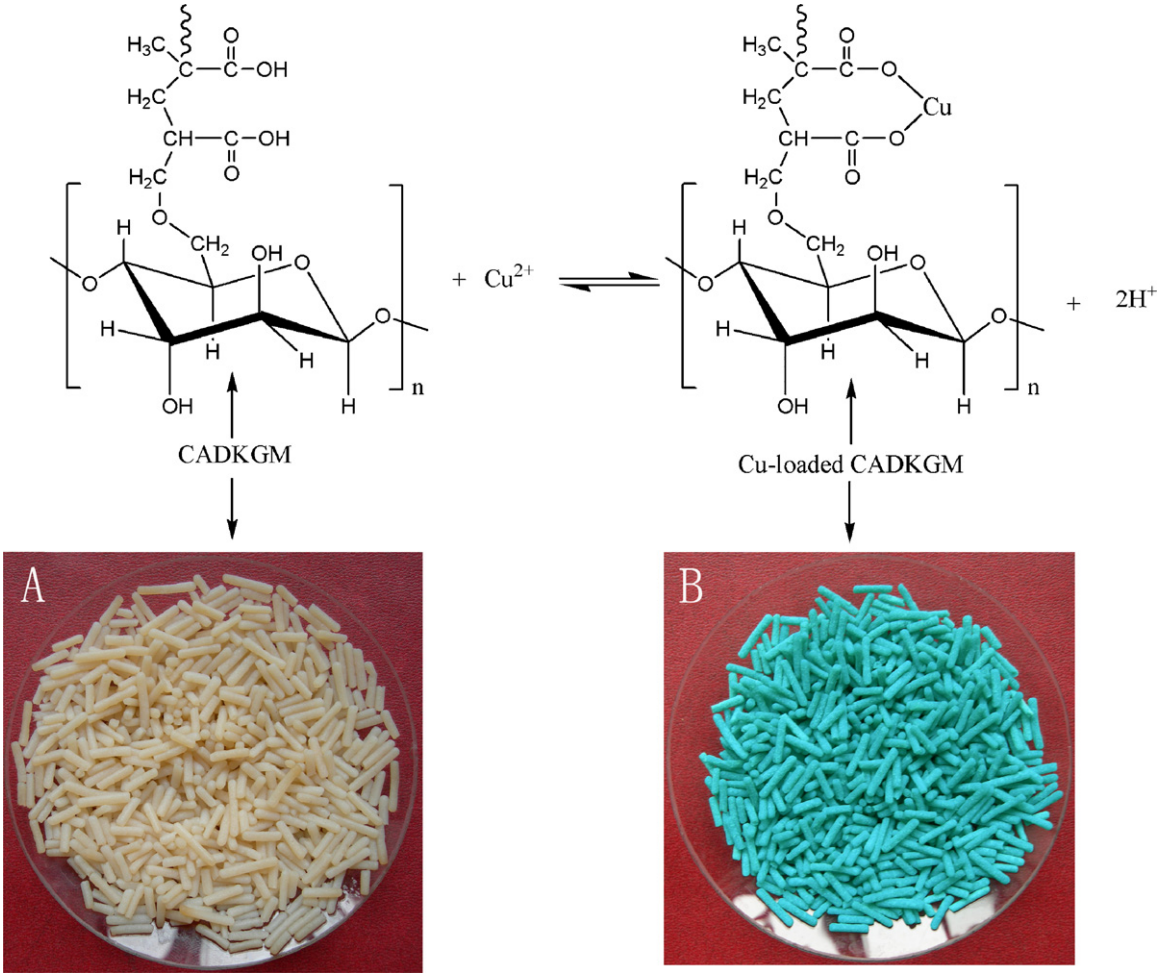

Fig. 7. The adsorption–desorption mechanism of Cu^{2+} ions on CADKGM.

cycle are given in Fig. 6(a). The adsorption curves from cycle 1 to 3 show a very similar shape. The column capacity of CADKGM was not affected by increase of reusable time and kept at almost the same value. Desorption cycles of Cu^{2+} ion from Cu-loaded CADKGM are shown in Fig. 6(b). Comparing the adsorption data with the desorption data, desorption efficiency was calculated as 98%. Moreover, this regeneration process can be repeated up to 10 times. After 10 cycles, the regenerated CADKGM adsorbents before and after adsorption of Cu^{2+} ions are shown in Fig. 7(A) and (B), respectively. The CADKGM bed did not settled down after 10 cycles. It indicated that CADKGM had good mechanic strength to support the bed due to remaining matrix structure of the TDKGM plastic. The adsorption–desorption mechanism of Cu^{2+} ions on CADKGM can be described in Fig. 7. The adsorption–desorption behavior of Cu^{2+} ions on CADKGM is much dependent on pH value of solution. At higher pH value, H^+ ions at lower concentration binding on negatively charged sites of CADKGM are exchanged by positively charged Cu^{2+} ions. On the contrary, at lower pH value, H^+ ions at higher concentration exchange with Cu^{2+} ions from the negatively charged sites of carboxylic acid groups on CADKGM. Therefore, adsorption–desorption Cu^{2+} ions process on CADKGM can be easily taken through pH adjustment of solution. After adsorption of Cu^{2+} ions on CADKGM, it is easy to regenerate and reuse again which make CADKGM a good candidate for adsorption of Cu^{2+} ions from wastewater.

4. Conclusion

Carboxylic acid functionalized deacetylated konjac glucomannan has been developed porous structure and good mechanical strength through traditional thermoplastic processing technology and was then chemically activated by sodium hydroxide. The column capacity of CADKGM remained relatively constant when the

parameters of bed height and flow rate were changed. However, the column capacity of CADKGM could evidently be improved with increase of the initial concentration. The maximum column capacity can reach 35.0 mg g^{-1} at higher Cu^{2+} ion concentration. The Thomas model was reasonably accurate in predicting experimental column capacity. CADKGM adsorbent can be regenerated and operated for multiple uses without any considerable loss in column capacity. This study identified CADKGM as a good candidate to be utilized for continuous removal of Cu^{2+} ions from aqueous solution.

Acknowledgement

This work was supported by National Key Technology R&D Program of China (No. 2007BAB18B08).

References

Ahmed, S. A. (2011). Batch and fixed-bed column techniques for removal of Cu(II) and Fe(III) using carbohydrate natural polymer modified complexing agents. *Carbohydrate Polymers*, *83*, 1470–1478.

Babel, S., & Kurniawan, T. A. (2003). Low-cost adsorbents for heavy metals uptake from contaminated water: A review. *Journal of Hazardous Materials*, *97*, 219–243.

Bailey, S. E., Olin, T. J., Bricka, R. M., & Adrian, D. D. (1999). A review of potentially low-cost sorbents for heavy metals. *Water Research*, *33*, 2469–2479.

Bohart, G. S., & Adams, E. Q. (1920). Some aspects of the behavior of charcoal with respect to chlorine. *Journal of the American Chemical Society*, *42*, 523–544.

Demirbas, A. (2008). Heavy metal adsorption onto agro-based waste materials: A review. *Journal of Hazardous Materials*, *157*, 220–229.

El Samrani, A. G., Lartiges, B. S., & Villieras, F. (2008). Chemical coagulation of combined sewer overflow: Heavy metal removal and treatment optimization. *Water Research*, *42*, 951–960.

Farooq, U., Kozinski, J. A., Khan, M. A., & Athar, M. (2010). Biosorption of heavy metal ions using wheat based biosorbents – A review of the recent literature. *Bioresource Technology*, *101*, 5043–5053.

Futalan, C. M., Kan, C. C., Dalida, M. L., Pascua, C., & Wan, M. W. (2011). Fixed-bed column studies on the removal of copper using chitosan immobilized on bentonite. *Carbohydrate Polymers*, *83*, 697–704.

Kose, T. E., & Ozturk, N. (2008). Boron removal from aqueous solutions by ion-exchange resin: column sorption–elution studies. *Journal of Hazardous Materials*, *152*, 744–749.

Kumar, U., & Bandyopadhyay, M. (2006). Fixed bed column study for Cd(II) removal from wastewater using treated rice husk. *Journal of Hazardous Materials*, *129*, 253–259.

Li, P. J., Wang, X., Allinson, G., Li, X. J., & Xiong, X. Z. (2009). Risk assessment of heavy metals in soil previously irrigated with industrial wastewater in Shenyang, China. *Journal of Hazardous Materials*, *161*, 516–521.

Liu, F., Luo, X. G., Lin, X. Y., Liang, L. L., & Chen, Y. (2009). Removal of copper and lead from aqueous solution by carboxylic acid functionalized deacetylated konjac glucomannan. *Journal of Hazardous Materials*, *171*, 802–808.

Liu, W., Yang, Y. S., Li, P. J., Zhou, Q. X., Xie, L. J., & Han, Y. P. (2009). Risk assessment of cadmium-contaminated soil on plant DNA damage using RAPD and physiological indices. *Journal of Hazardous Materials*, *161*, 878–883.

Lu, X. W., Wang, L. J., Lei, K., Huang, J., & Zhai, Y. X. (2009). Contamination assessment of copper, lead, zinc, manganese and nickel in street dust of Baoji, NW China. *Journal of Hazardous Materials*, *161*, 1058–1062.

Matlock, M. M, Howerton, B. S., & Atwood, D. A. (2002). Chemical precipitation of heavy metals from acid mine drainage. *Water Research*, *36*, 4757–4764.

Nayek, S., Gupta, S., & Saha, R. N. (2010). Metal accumulation and its effects in relation to biochemical response of vegetables irrigated with metal contaminated water and wastewater. *Journal of Hazardous Materials*, *178*, 588–595.

O'Connell, D. W., Birkinshaw, C., & O'Dwyer, T. F. (2008). Heavy metal adsorbents prepared from the modification of cellulose: A review. *Bioresource Technology*, *99*, 6709–6724.

Pehlivan, E., & Altun, T. (2007). Ion-exchange of Pb^{2+}, Cu^{2+}, Zn^{2+}, Cd^{2+}, and Ni^{2+} ions from aqueous solution by Lewatit CNP 80. *Journal of Hazardous Materials*, *140*, 299–307.

Peng, J. F, Song, Y. H., Yuan, P., Cui, X. Y., & Qiu, G. L. (2009). The remediation of heavy metals contaminated sediment. *Journal of Hazardous Materials*, *161*, 633–640.

Qaiser, S., Saleemi, A. R., & Umar, M. (2009). Biosorption of lead from aqueous solution by Ficus religiosa leaves: Batch and column study. *Journal of Hazardous Materials*, *166*, 998–1005.

Sang, Y. M., Gu, Q. B., Sun, T. C., Li, F. S., & Liang, C. Z. (2008). Filtration by a novel nanofiber membrane and alumina adsorption to remove copper(II) from groundwater. *Journal of Hazardous Materials*, *153*, 860–866.

Shi, W. Y., Shao, H. B., Li, H., Shao, M. A., & Du, S. (2009). Progress in the remediation of hazardous heavy metal-polluted soils by natural zeolite. *Journal of Hazardous Materials*, *170*, 1–6.

Sud, D., Mahajan, G., & Kaur, M. P. (2008). Agricultural waste material as potential adsorbent for sequestering heavy metal ions from aqueous solutions – a review. *Bioresource Technology*, *99*, 6017–6027.

Sunarso, J., & Ismadji, S. (2009). Decontamination of hazardous substances from solid matrices and liquids using supercritical fluids extraction: a review. *Journal of Hazardous Materials*, *161*, 1–20.

Tabakci, M., & Yilmaz, M. (2008). Sorption characteristics of Cu(II) ions onto silica gel-immobilized calix[4]arene polymer in aqueous solutions: Batch and column studies. *Journal of Hazardous Materials*, *151*, 331–338.

Vijayaraghavan, K., & Yun, Y. S. (2008). Bacterial biosorbents and biosorption. *Biotechnology Advances*, *26*, 266–291.

Wan Ngah, W. S., Teong, L. C., & Hanafiah, M. A. K. M. (2011). Adsorption of dyes and heavy metal ions by chitosan composites: A review. *Carbohydrate Polymers*, *83*, 1446–1456.

Wang, J. L., & Chen, C. (2009). Biosorbents for heavy metals removal and their future. *Biotechnology Advances*, *27*, 195–226.

Wei, B. G., & Yang, L. S. (2010). A review of heavy metal contaminations in urban soils, urban road dusts and agricultural soils from China. *Microchemical Journal*, *94*, 99–107.

Wu, F. C., Tseng, R. L., & Juang, R. S. (2010). A review and experimental verification of using chitosan and its derivatives as adsorbents for selected heavy metals. *Journal of Environmental Management*, *91*, 798–806.

Wu, G., Kang, H. B., Zhang, X. Y., Shao, H. B., Chu, L. Y., & Ruan, C. J. (2010). A critical review on the bio-removal of hazardous heavy metals from contaminated soils: Issues, progress, eco-environmental concerns and opportunities. *Journal of Hazardous Materials*, *174*, 1–8.

Xu, C. G, Luo, X. G., Lin, X. Y., Zhuo, X. R., & Liang, L. L. (2009). Preparation and characterization of polylactide/thermoplastic konjac glucomannan blends. *Polymer*, *50*, 3698–3705.